Toward Automated Manufacturing of RF Coils: Microstrip Resonators for 4.7 T Using 3D-printed Dielectrics and Conductors

Saeed Javidmehr[a], Adam M. Maunder[a], Mojgan Daneshmand[a*], Nicola De Zanche[b,c*]

a) Department of Electrical and Computer Engineering at the University of Alberta, Edmonton, AB, Canada
b) Alberta Health Services, Cross Cancer Institute, Edmonton, AB, Canada
c) Department of Oncology (Division of Medical Physics), University of Alberta, Edmonton, AB, Canada

Published in

Applied Magnetic Resonance 50(5): 663–675 (2019)

DOI: 10.1007/s00723-018-1108-9

*** Corresponding authors:**

Nicola De Zanche
Department of Medical Physics
Cross Cancer Institute
11560 University Avenue
Edmonton, Alberta, Canada
T6G 1Z2
Telephone: 780-989-8155
Fax: 780-432-8615
Email: dezanche@ualberta.ca

Mojgan Daneshmand
Department of Electrical and Computer Engineering
University of Alberta
DICE 11-324
Edmonton, Alberta, Canada
T6G 1H9
Telephone: 780-492-7351
Email: daneshmand@ualberta.ca

ABSTRACT

Microstrip transmission line (MTL) resonators are widely used as radio frequency (RF) transceiver coils in high-field MR imaging. Typically, discrete capacitors are used to tune the MTL resonators to the Larmor frequency, and to match to the 50 Ω characteristic impedance of the RF chain. The cost, availability, and labour-intensive work of soldering capacitors on each coil contributes significantly to the expense of RF coil arrays for MRI; therefore, a manufacturing method with lower cost and fewer processing steps is desirable. The additive manufacturing method of rapid prototyping offers a new method to build custom-designed MTL resonators with reduced fabrication steps and, potentially, cost. This feasibility study explores fused deposition modelling to 3D print the MTL resonator structure simultaneously with matching/tuning capacitors and conductors. Typical low-cost 3D printers are capable of printing only polymers, not metal and polymer printing in one machine. In this work, a low-cost 3D printer was modified by adding the capability to print conductive ink and used to print MTL resonators with monolithic parallel-plate capacitors. These integrated capacitors eliminate the repetitive work of soldering, and tuning is achieved by trimming the capacitor plates. Additionally, 3D printing allows unconventional designs that minimize the amount of dielectric below the microstrip and therefore losses in the substrate. Resulting SNR values using ink conductors are within 30% of those achieved with copper despite a resistivity that is two orders of magnitude higher. This performance gap can be addressed by using newer inks that have much lower resistivity.

Keywords—3D printed circuits, additive manufacturing, fused deposition modelling, microstrip transmission line resonator, transceive array element, conductive ink

INTRODUCTION

Radio-frequency (RF) coil arrays provide higher signal to noise ratio (SNR) than volume coils and in transmission they also allow optimization of transmit B_1 uniformity and specific absorption rate (SAR) [1, 2]. The greater is the number of channels the greater the degrees of freedom available to achieve the desired field control. However, if a large number of array elements is required the coil elements should be made using a coil geometry that is readily manufactured. The microstrip transmission line (MTL) resonator is a common array element which consists of a length of microstrip transmission line separated from a ground plane by a dielectric substrate, typically with tuning capacitors at both ends [3-5]. Compared to loop coils they have stable resonance [6], lower coupling between array elements [6, 7], and lower radiation losses by using a ground plane. Feeding can be achieved through a matching capacitor at one end or through a central balanced connection [8]. Arrays of such elements are efficient [5, 9] and provide reduced coupling between transmit elements compared to loop coils [10, 11], while allowing uniform excitations [11]. Advantages of microstrip coils over standard loops are a consequence of lower E-field losses and more confined electromagnetic fields [10, 12].

In standard RF coil construction, copper traces are laid down by hand, e.g., using self-adhesive copper tape, or chemically etched using printed circuit board technology. Costly discrete tuning and matching capacitors are manually soldered onto the coil to tune the coil to the Larmor frequency and match it to 50 Ω. Replacing this labor-intensive and time consuming process with an automated, rapid-prototyping technology could eliminate the tedious repetition required for array construction, and possibly also reduce the total cost and time. Avoiding discrete capacitors would also contribute to reducing manufacturing costs. It has been recently shown that 3D printing of polymer substrates and silver nanoparticle inks can be used to build RF devices [13]. This technology replaces the traditional fabrication methods, and uses an additive manufacturing technique to build a 3D device by laying down successive layers of structural material. Designs are created in standard RF simulation or computer-aided design (CAD) software. We introduce

this flexible, cost-effective approach to custom MRI coil fabrication using an economical desktop 3D printer. Within few hours, and with minimal user intervention, an MR-compatible MTL resonator is fabricated with 3D-printed parallel plate capacitors monolithically integrated. A further advantage of 3D printing technology in MRI coil design is that the amount of dielectric material can be minimized by creating hollow spaces in regions of high electric fields, lowering the resonator's losses thus increasing the coil's efficiency and SNR.

Rapid prototyping machines vary in cost based on their printing resolution, printing process, materials used, speed, etc. Additive manufacturing (or 3D printing) has become popular in recent years due to the decreasing cost of fused deposition modelling, in which molten material (typically a thermoplastic) is extruded and deposited in layers to create the desired part. A typical low-cost (~$2,000 US) desktop 3D printer found in many RF coil labs has only one extruder to deposit the polymer onto the print bed. In this feasibility study, we retrofit such a printer with the capability of printing conductive ink and fabricate various MTL resonators for 4.7 T (200.4 MHz) using three different dielectric materials and copper tape or silver ink conductors. Their electrical and imaging performance is compared to that of a standard low-loss foam MTL resonator in terms of quality factor, efficiency and signal to noise ratio (SNR).

METHODS

Design

The MTL resonator geometry, shown in Figure 1, includes monolithically-integrated capacitors and dielectric substrate (green). Conductive material (copper tape or silver ink) is shown in red. The resonator's resonant frequency is adjusted using parallel plate capacitors at both ends of the section of microstrip. The ground plane is positioned on top of the 1-mm-thick flat base, instead of below it, to minimize the effective permittivity in the area between the signal line and ground. The 13-cm-long signal line is supported 1 cm above the ground plane with three uniformly-spaced vertical dielectric cylinders. The microstrip's

width/height ratio is chosen equal to unity to optimize B_1 penetration [14]. Integrated capacitors consist of 3D-printed dielectric between conductive plates thus eliminating the need for expensive discrete capacitors, and the time-consuming connection process (soldering). Shunt capacitors (C_p in Figure 1, two adjacent rectangles of dimensions $W_{p1}\times L_{p1}$, and $W_{p2}\times L_{p2}$) protrude from both ends of the resonator and a series capacitor, C_s, ($W_s\times L_s$) is connected to one side for matching. An array of 8 of these elements would be appropriate for imaging the human head.

<Figure 1>

Materials

The following 3D printer polymers are used: Polylactic Acid (PLA) and Acrylonititrile Butadiene Styrene (ABS) (Reprapper Tech, Hong Kong); and UV-curing acrylic resin photopolymer (Objet Verogray RGD850, Stratasys). The favorable MRI properties of 3D printed PLA and ABS have been investigated in [15] where it was found that both materials have magnetic susceptibility very close to that of water while emitting zero observable NMR signals down to an echo time of 5.2 ms.

Copper tape (MasterFoil Plus, VentureTape, USA) and conductive silver ink (Ag-610, Applied Ink Solutions, USA) are used for conductive lines, capacitors and ground layers, and their performance is compared to that of a standard MTL resonator made with copper strips on low loss foam substrate (51HF, Rohacell, Evonik, Germany) with identical dimensions.

Material Characterization and Tuning

Because the printed polymers are partially air-filled, physical bench-top measurements were used to fine-tune the corresponding complex permittivities in simulations performed with High Frequency Structure Simulator (HFSS, ANSYS, USA). An initial version of Figure 1a) was modeled without shunt and series capacitors at the ends. Two lumped ports were connected at the ends of the microstrip and scattering (S) parameters were simulated with initial permittivity $\varepsilon_r = 2$ and loss factor $\tan\delta = 0.02$ for both ABS and PLA. The S parameters were imported for network analysis into Advanced Design System (ADS, Keysight,

Santa Rosa, USA) to determine the shunt and series capacitors needed to match Z_{in} to 50 Ω (return loss of 30 dB or better) at 200.4 MHz [16].

With these initial estimates of capacitor plate dimensions, prototypes were printed with each dielectric (c.f. Fabrication), and bench measurements of resonant frequency and quality factor were made. The frequencies from measurements and simulations differed by up to 20 MHz for ABS and PLA, and thus the permittivity and loss tangent of the dielectric were adjusted (Table 1) in the HFSS simulation to match the measurements. With these values, the capacitor plate dimensions were then adjusted (Table 2) to tune and match the coil at 200.4 MHz. Because the printed material is not perfectly solid but contains air inclusions, the volume fraction of air and polymer (Table 1) was calculated from the effective and literature values of permittivity as described in Ref. [17].

Table 1: Effective complex permittivity determined by adjusting it to match simulation results to benchtop measurements. Since the 3D printing process introduces air spaces within the material, the volume fraction of air/polymer was calculated based on the permittivity reported in the literature for the solid material and that of air.

Material Name	*Complex Permittivity*	*Volume Fraction (f)*	*Reported Permittivity*
PLA	1.24(1+*i*·0.005)	0.19	3 [13, 18]
ABS	1.34(1+*i*·0.008)	0.27	2.87
UV-resin	2.0(1+*i*·0.026)	0.46	4.5 [19]

Table 2: Tuning and matching capacitor dimensions for ABS and PLA (*).

Capacitors	**Width (cm)**	**Length (cm)**	**Dielectric Thickness (mm)**	**Capacitance (pF)**
Series C_s	$W_s = 1.5$	$L_s = 1.5$	t=1	3.8
Shunt C_p	$W_{p1} = 2.9,$ $W_{p2} = 1.1$	$L_{p1} = 1.9,$ $L_{p2} = 2.56, 2.7^*$	t=1	19.5

The sheet resistance of silver ink cured on a glass substrate was measured using a four point probe (Pro4 4000, Signatone, Gilroy, USA). The ink was dispensed and dried at room temperature for 5 to 10 minutes according to the manufacturer's instructions. Additional curing can be done using forced air or by placing the printed parts on a heated bed if the substrate allows. Curing at 200°C was repeated until the measured resistance decreased less than 10% from the original value. A two-dimensional surface topography profiler (Alpha Step IQ, KLA-Tencor, Malpitas, USA) was used to measure the thickness, $d = 10\ \mu m$, of the ink, from which the bulk resistivity can be determined. Results are compared to values for copper foil inTable 3.

Table 3: measured resistivity and sheet resistance of silver ink compared to literature values for copper foil (32 μm thick, room temperature) [20].

Conductive Material	*Sheet Resistance* ($\boldsymbol{R_s}$, $\Omega/\boldsymbol{m}$)	*Bulk Resistance (Ω-m)*
Silver-ink Ag-610	34.7×10^{-2}	347×10^{-8}
Copper foil	0.052×10^{-2}	1.68×10^{-8}

Fabrication

The dielectric structures were fabricated using different printers depending on the material chosen for a particular coil. A desktop 3D printer (X-series, Machina Corp., Edmonton, Canada) was used to print PLA and ABS and an Objet Eden350V (Stratasys, Eden Prairie, USA) was used to print UV-curable resin (Objet Verogray RGD850, Stratasys). This material provides better mechanical performance than ABS or PLA, and a sacrificial support material can also be printed and subsequently removed with water and acetone. The complete structure can therefore be printed simultaneously, unlike the X-series printer where the signal line and the ground plane are printed separately and snapped together afterwards. Printing times are of the order of a few minutes and vary depending on the printer used and dimensions and complexity of the structure.

The X-series printer was modified to deposit the conductive silver ink on the dielectric substrates by adding a second printing head consisting of a syringe (Nordson, Westlake, USA) with a 600 μm diameter tip

(chosen based on pressure and viscosity) connected to a programmable pressure regulator (UltimusV, Nordson) (Figure 2). With such extrusion printers, the infill density must be sufficiently high to avoid the formation of gaps large enough for ink to flow into the polymer layers. In the regions of the capacitor dielectric this can cause short circuits and failure of the resonator.

<Figure 2>

The printer's numerical control program file (g-code) was modified (Figure 3) to assign printing paths for the syringe, while disabling the standard print head (extruder) by setting its temperature to zero so that polymer is not extruded. Conversely, the heat bed temperature is manually set to 60°C to increase adhesion between its surface and the part on which ink is to be printed. Offsets (x=4.1 cm and z=1–12.3 mm) are entered in the g code to account for the different locations of the syringe compared to the extruder head. The z offset depends on which side of the parts the ink is printed.

<Figure 3>

A skirt is first printed on the print bed (Figure 4) to confirm alignment of the part with the coordinates that are used for printing ink. Ink deposition (Figure 5) begins with the ground plane, followed by top of the signal line including capacitors, and finally the two vertical ground connections (walls). After printing ink on the top, the signal line is flipped to print on the bottom of the capacitors. The pieces are assembled, and a small amount of conductive silver epoxy (8331-14G, M.G. Chemicals, Canada) is used to attach the walls between the bottom of the capacitors and ground. The printing speed and dispensing pressure are determined experimentally to achieve uniform flow with the viscosity of the specific ink used. For the Ag-610 ink the dispensing pressure was set to 61 kPa for initial flow (since the ink might dry inside the tip and higher pressure is needed to unclog it) and 34 kPa for normal continuous printing. After drying at room temperature, final curing of the ink was done for 1 h at 60°C for PLA and 100°C for ABS.

<Figure 4>

<Figure 5>

Several versions of these resonators were fabricated (Figure 6 and Table 4) using various combinations of dielectrics and conductors. Performance was compared to that of a standard MTL resonator (resonator #6) made with copper strips, porcelain capacitors (ATC 100B, American Technical Ceramics, USA) and trimmer capacitors (TZ03 series, Murata Electronics, Japan) on low-loss Rohacell foam [5]. Resonators 1 and 3 are fully printed using silver ink on ABS and PLA, respectively, while resonators 2, 4, and 5 use copper conductors but no discrete capacitors or trimmers.

<Figure 6>

Table 4: Summary of resonator construction combinations.

Resonator	**dielectric**	**conductor**	**Capacitors**
Res-1	ABS	Ag-610 ink	3D-printed
Res-2	ABS	Cu	3D-printed
Res-3	PLA	Ag-610 ink	3D-printed
Res-4	PLA	Cu	3D-printed
Res-5	UV Resin	Cu	3D-printed
Res-6	Foam	Cu	ATC + Trimmer

Warping of the microstrip line due to shrinkage of the ink was observed most noticeably with the PLA material (resonator #3). In future designs this can be reduced by strengthening the underside of the microstrip (e.g., by adding ribs, fins and/or trusses); by reducing temperature gradients and air flow from the environment by curing within an enclosed chamber; and/or by using a room-temperature curing ink (e.g., Voxel8 silver ink, Voxel8, Somerville, MA).

Connections to coaxial cables for resonators with copper conductors were achieved by soldering an SMA-type connector between the bottom plate of the series capacitor (Cs) and the ground plane. For resonators with ink conductors, soldering cannot be used because the ink degrades at soldering temperatures (the

dielectric thermoplastic substrates also melt). The solution was to solder the SMA connector to small pieces of copper tape which are then connected to the bottom plate of the series capacitor and to the ground plane using small amounts of conductive ink.

Measurements

Measurements and simulations were performed with each individual resonator placed 1 cm above a 36×26×11 cm^3 phantom filled with 3.6 g/ℓ NaCl and 1.96 g/ℓ $CuSO_4 \cdot 5H_2O$ to simulate the human body (ε_r=76, σ=0.8 S/m) [21]. For geometrical reference the phantom also contains a perforated plastic panel of ~13 mm squares at a depth of 25 mm.

Measurements of S_{11} were performed on a ZVL3 vector network analyzer (Rohde & Schwarz, Germany) following a Short-Open-Load-Thru (SOLT) calibration to account for cable losses and phase shifts [22]. The area of the parallel plate capacitors was made slightly larger to allow tuning to 200.4 MHz and matching to a 15 dB return loss or better by trimming the capacitor plates' lengths and widths using a hobby knife. Loaded (Q_l) and unloaded (Q_u) quality factors are measured according to Ref. [23] and used to compare the performance of RF coils [24].

Gradient-echo images (T_R/T_E = 50/5 ms, flip angle = 10°, bandwidth = 391 Hz/pixel, acquisition matrix 256×128, FOV = 30×30 cm, 1 average, slice thickness = 5 mm) were acquired on a 4.7 T Varian Inova system to compare SNR performance of the individual resonators. A transmit-receive switch was used to allow each resonator to both transmit excitation pulses and to receive the resulting MR signal. Maps of SNR were calculated from the complex images by dividing image magnitude by the standard deviation of the background noise measured in a rectangular region (256×30 pixels) outside the phantom.

RESULTS AND DISCUSSION

Maps of SNR in sagittal and coronal orientations (2.5 cm below the top of the phantom) are shown in Figure 7. Efficiency $\eta = 1 - Q_l/Q_u$ [25] values are listed in Table 5 along with return loss (S_{11}) and average SNR in three sagittal slices (one central and two offset ±1.5cm; 13×4 cm^2 area).

The efficiency of 3D-printed resonators with ink conductors or UV-curing resin is significantly lower than that of a standard resonator made with copper, Rohacell foam dielectric, and discrete capacitors. Conversely, resonators made with PLA and ABS show comparable Q and efficiency to those of the standard resonator. These results are consistent with the much higher losses of the UV-curing resin compared to PLA and ABS (Table 1). Even though silver ink has a resistivity that is two orders of magnitude higher than that of copper (Table 3), the consequent reduction in image SNR is very limited because in the unloaded standard resonator the dominant loss mechanism is probably dielectric loss in the integrated capacitors. Alternative inks with lower resistivity have subsequently been found (PChem, PFI-722 silver nanoparticle ink, 5.3×10^{-8} Ωm; Voxel8 silver ink, 3.3×10^{-8} Ωm) that will provide conductivity nearly equal that of copper (indeed better than many metals).

<Figure 7>

Table 5: Measurement results for return loss ($|S_{11}|$), loaded and unloaded Q factors, square root of efficiency, and SNR average over three sagittal slices for each MTL resonator in Table 4.

Resonator number	Construction	Return loss $\lvert S_{11}\rvert$	$Q_{unloaded}$	Q_{loaded}	$\sqrt{\eta}$	Average SNR
1	ABS-ink	-22 dB	28.5	22.6	0.455	53.1
2	ABS-cu	-30 dB	79.3	33.1	0.763	59.4
3	PLA-ink	-22 dB	29.0	18.2	0.610	29.4
4	PLA-cu	-30 dB	98.9	29.8	0.836	41.5
5	Resin-cu	-15 dB	40.4	28.1	0.552	40.5
6	Foam-cu	-30 dB	123	51.4	0.763	42.4

Agreement between measured SNR values and what would be expected based on efficiency ($SNR \propto iSNR\sqrt{\eta}$, where *iSNR* is the intrinsic SNR achievable in absence of coil losses) [24] is not exact, but nevertheless shows that the ink conductor leads to a limited SNR loss of 10–30% relative to that of the corresponding copper resonator (resonators 1 vs. 2 and 3 vs. 4). Discrepancies between bench and imaging measurements are probably due to experimental conditions that are difficult to control, such as achieving consistent flip angle calibration in the presence of large RF field gradients, or differences in losses between the bench and the scanner. These results are, however, sufficient to conclude that future work should focus on the use of higher-conductivity inks while avoiding the use of the UV-curing resin.

CONCLUSION

This feasibility study demonstrates the potential of utilizing 3D printing technology to fabricate MTL resonators for MR in an automated manner directly from CAD data used in simulations. Parallel plate capacitors are monolithically integrated and conductors are printed using conductive silver ink. Multiple labour-intensive production steps such as soldering discrete capacitors in the traditional construction method are eliminated, thus potentially reducing the costs and assembly time of traditional MTL resonator fabrication. The initial characterization of the complex permittivity of the printed material yields accurate simulations and prevents design iterations. In this feasibility study a low-cost 3D printer is modified to print ink, allowing dielectric and conductive portions to be printed with the same machine. Not all 3D printing materials are suitable for RF devices, and we found that ABS and PLA have lower losses than the UV-curing resin at MRI frequencies even though the resin is mechanically superior. These losses are significant in the dielectric of integrated capacitors where electric fields are strongest. Nevertheless, the amount of dielectric (and thus additional dielectric losses) used in the rest of the resonator can be minimized by designing a hollow support structure for the microstrip. Resonators with ink conductors do exhibit lower efficiency and SNR compared to those made of copper because of the higher resistivity of the ink.

However, this gap in performance is quite limited compared to the wide difference in resistivity, and will be mostly eliminated by using inks with lower resistivity.

Future work includes exploring the high voltage limits of printed MTL resonators, as well as investigating materials with lower RF losses and printed tunable capacitors such as those described in Refs. [26, 27]. Future work also includes assembling multiple resonators into an array, as well as investigating mechanical stability of the assembly, thermal stability under high powers, and gradient eddy current performance.

ACKNOWLEDGMENTS

The authors wish to acknowledge CMC Microsystems for software access and Machina Corp. for assistance with their 3D printer. We thank Peter Šereš for assistance with imaging measurements, and Sabreen Khan for proofreading. We also thank Mr. Herbert Dexel for assistance with setup of the pressure regulator and Evonik Inc. for providing the Rohacell foam.

FUNDING

This work was supported by the Canada Research Chairs Program and by the Natural Sciences and Engineering Research Council (Canada).

FIGURE CAPTIONS

Figure 1: a) Rendering of the 3D-printed partially air-filled microstrip coil. Dimensions for shunt and series capacitor plates are listed in Table 2. Green represents the polymer dielectric substrate and red the conductive material (copper tape or silver ink). Capacitors at both ends provide tuning and matching. b) Equivalent circuit model of the MTL resonator with tuning and matching capacitors.

Figure 2: desktop 3D printer (X-series, Machina Corp) modified to deposit conductive ink. Compressed air (pressure of 0.62 MPa) is fed into the dispenser. Uniform flow is achieved by using a regulator to maintain an air pressure of 35 to 60 kPa to extrude the ink.

Figure 3: Printing instructions ("g-code") for 3D printer modified for ink deposition. The modification involves: initial set-up (home coordinates, syringe offsets), layer instructions (polymer extrusion disabled), and conclusion (turns heat bed off and ends the job).

Figure 4: 3D printing of conductive ink on (a) the PLA signal line with capacitors, and (b) ABS ground plane and (c) bottom side of capacitors. A skirt is printed on the print bed as a reference for correct alignment of the parts.

Figure 5: Ink deposition process begins with the ground plane, top of the signal line including capacitors, and ground connections (walls). The signal line is then flipped to print ink on the bottom side of the capacitors.

Figure 6: Resonators fabricated using the material combinations listed in Table 4. Resonators 1–5 use monolithic 3D printed parallel plate capacitors. Resonators with conductive ink are printed on ABS (1) and PLA (3). Resonator 6 is built on Rohacell foam as a performance standard for comparison.

Figure 7: Coronal (a) and sagittal (b) SNR maps of each resonator (see descriptions in Table 4). Images are from an 8×15 cm^2 FOV for coronal and a 4×15 cm^2 FOV for sagittal maps. Higher peak values in the sagittal maps are due to orientation and depth of the coronal slices (approximate location shown by dashed white lines). The ~13 mm square grid pattern is due to a perforated plastic panel inside the phantom.

REFERENCES

[1] U. Katscher and P. Bornert, "Parallel RF transmission in MRI," *NMR Biomed,* vol. 19, pp. 393-400, May 2006.

[2] P. Vernickel, P. Roschmann, C. Findeklee, K. M. Ludeke, C. Leussler, J. Overweg*, et al.*, "Eight-channel transmit/receive body MRI coil at 3T," *Magn Reson Med,* vol. 58, pp. 381-9, Aug 2007.

[3] Y. Pang, Z. Xie, D. Xu, D. A. Kelley, S. J. Nelson, D. B. Vigneron*, et al.*, "A dual-tuned quadrature volume coil with mixed λ/2 and λ/4 microstrip resonators for multinuclear MRSI at 7T," *Magnetic Resonance Imaging,* vol. 30, pp. 290-298, 11/03 2012.

[4] X. Zhang, X. H. Zhu, and W. Chen, "Higher-order harmonic transmission-line RF coil design for MR applications," *Magn Reson Med,* vol. 53, pp. 1234-9, May 2005.

[5] Z. Xiaoliang, K. Ugurbil, R. Sainati, and C. Wei, "An inverted-microstrip resonator for human head proton MR imaging at 7 tesla," *IEEE Transactions on Biomedical Engineering,* vol. 52, pp. 495-504, 2005.

[6] B. Wu, C. Wang, J. Lu, Y. Pang, S. J. Nelson, D. B. Vigneron*, et al.*, "Multi-channel microstrip transceiver arrays using harmonics for high field MR imaging in humans," *IEEE Trans Med Imaging,* vol. 31, pp. 183-91, Feb 2012.

[7] X. Zhang, Y. Liao, X.-H. Zhu, and W. Chen, "An MTL coil array with a broad frequency tuning range for ultra-high field human MR applications from 3T to 7T," *Proc. Intl. Soc. Mag. Reson. Med.,* vol. 11, p. 1602, 2004.

[8] D. O. Brunner, N. D. Zanche, J. Froehlich, D. Baumann, and K. P. Pruessmann, "A symmetrically fed microstrip coil array for 7T," *Proc. Intl. Soc. Mag. Reson. Med.,* vol. 15, 2007.

[9] X. Zhang, K. Ugurbil, and W. Chen, "A microstrip transmission line volume coil for human head MR imaging at 4T," *J Magn Reson,* vol. 161, pp. 242-51, Apr 2003.

[10] G. Adriany, E. J. Auerbach, C. J. Snyder, A. Gözübüyük, S. Moeller, J. Ritter*, et al.*, "A 32-Channel Lattice Transmission Line Array for Parallel Transmit and Receive MRI at 7 Tesla," *Magnetic Resonance in Medicine,* vol. 63, pp. 1478-1485, 2010.

[11] G. Adriany, P. F. Van de Moortele, F. Wiesinger, S. Moeller, J. P. Strupp, P. Andersen*, et al.*, "Transmit and receive transmission line arrays for 7 Tesla parallel imaging," *Magn Reson Med,* vol. 53, pp. 434-45, Feb 2005.

[12] R. F. Lee, C. R. Westgate, R. G. Weiss, D. C. Newman, and P. A. Bottomley, "Planar Strip Array (PSA) for MRI," *Magnetic Resonance in Medicine,* vol. 45, pp. 673-683, 2001.

[13] M. Ahmadloo and P. Mousavi, "Application of novel integrated dielectric and conductive ink 3D printing technique for fabrication of conical spiral antennas," in *IEEE Antennas and Propagation Society International Symposium*, 2013, pp. 780-781.

[14] Y. Seo, "Design of microstrip-based surface coils for low-field small-bore MR applications," *Concepts in Magnetic Resonance Part B: Magnetic Resonance Engineering,* vol. 41B, pp. 111–119, 2012.

[15] K. H. Herrmann, C. Gartner, D. Gullmar, M. Kramer, and J. R. Reichenbach, "3D printing of MRI compatible components: why every MRI research group should have a low-budget 3D printer," *Med Eng Phys,* vol. 36, pp. 1373-80, Oct 2014.

[16] J. Mispelter, M. Lupu, and A. Briguet, *NMR Probeheads for Biophysical and Biomedical Experiments: Theoretical Principles & Practical Guidelines*: Imperial College Press, 2006.

[17] Q. X. Yang, W. Luo, S. Rupprecht, Z. Herse, C. Sica, J. Wang*, et al.*, "RF Field Enhancement with High Dielectric Constant (HDC) Pads in a Receive Array Coil at 3.0 T," *Journal of magnetic resonance imaging : JMRI,* vol. 38, pp. 435-440, 01/04 2013.

[18] T. Nakagawa, T. Nakiri, R. Hosoya, and Y. Tajitsu, "Electrical properties of biodegradable polylactic acid film," *IEEE Transactions on Industry Applications,* vol. 40, pp. 1020-1024, 2004.
[19] S. J. Park and F. L. Jin, "Synthesis and characterization of UV-curable acrylic resin containing fluorine groups," *Polymer International,* vol. 54, pp. 705-709, 2004.
[20] J. Rumble, *Handbook of Chemistry and Physics*. Boca Raton, FL, USA: CRC Press, 2017.
[21] J. G. Och, G. D. Clarke, W. T. Sobol, C. W. Rosen, and S. K. Mun, "Acceptance testing of magnetic resonance imaging systems: Report of AAPM Nuclear Magnetic Resonance Task Group No. 6," *Medical Physics,* vol. 19, pp. 217-229, 1992.
[22] H. Heuermann, "GSOLT: the calibration procedure for all multi-port vector network analyzers," in *IEEE International Microwave Symposium Digest*, 2003, pp. 1815-1818.
[23] A. Yahya, N. De Zanche, and S. Allen Peter, "A dual-tuned transceive resonator for $^{13}C^{1}H$ MRS: two open coils in one," *NMR in Biomedicine,* vol. 26, pp. 533-541, 2013.
[24] W. A. Edelstein, G. H. Glover, C. J. Hardy, and R. W. Redington, "The intrinsic signal-to-noise ratio in NMR imaging," *Magnetic Resonance in Medicine,* vol. 3, pp. 604-618, 1986.
[25] P. Mansfield and P. Morris, *NMR imaging in biomedicine*: Academic Press, 1982.
[26] A. R. Horch and J. C. Gore, "3D-printed RF Coils For Solution-state NMR: Towards Low-cost, High-throughput Arrays," *Proc. Intl. Soc. Mag. Reson. Med.,* vol. 23, p. 853, 2015.
[27] A. R. Horch and J. C. Gore, "3D-printed RF Probeheads for Low-cost, High-throughput NMR," *Proc. Intl. Soc. Mag. Reson. Med.,* vol. 24, p. 2147, 2016.

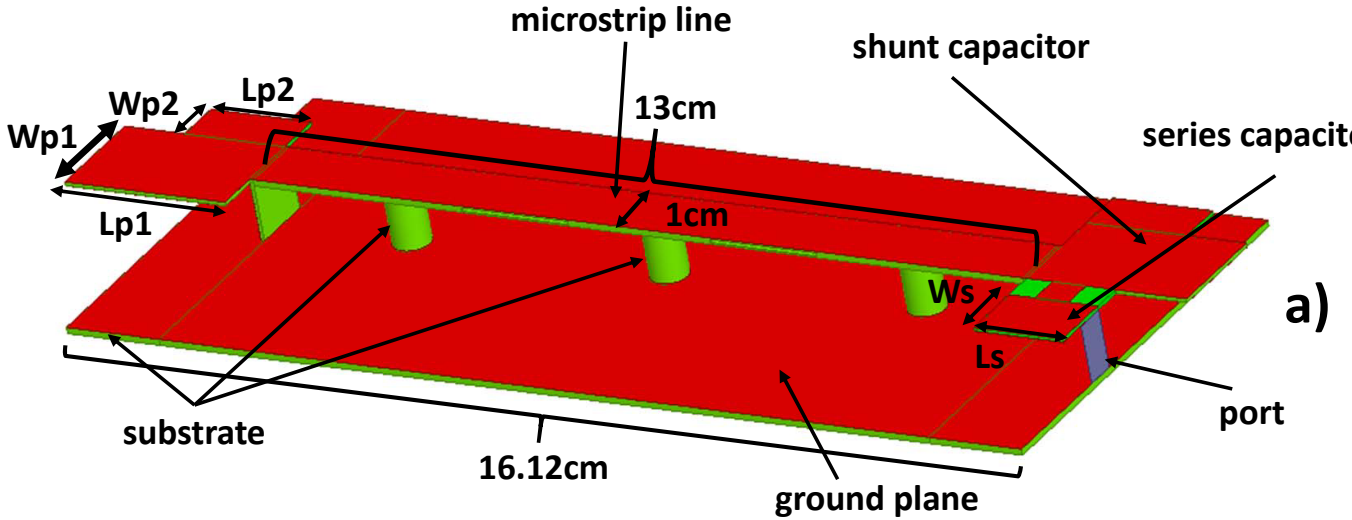
microstrip line
shunt capacitor
Wp2
Lp2
13cm
Wp1
series capacitor
Lp1
1cm
Ws
a)
Ls
port
substrate
16.12cm
ground plane

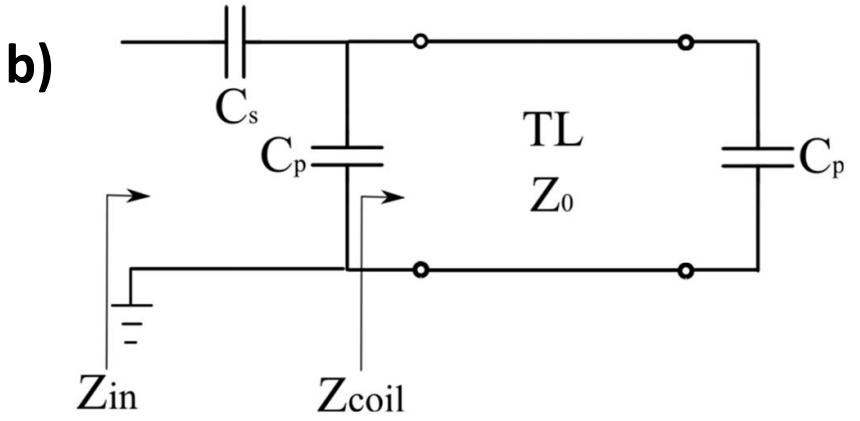
b)
Cs
Cp
TL
Z0
Cp
Zin
Zcoil

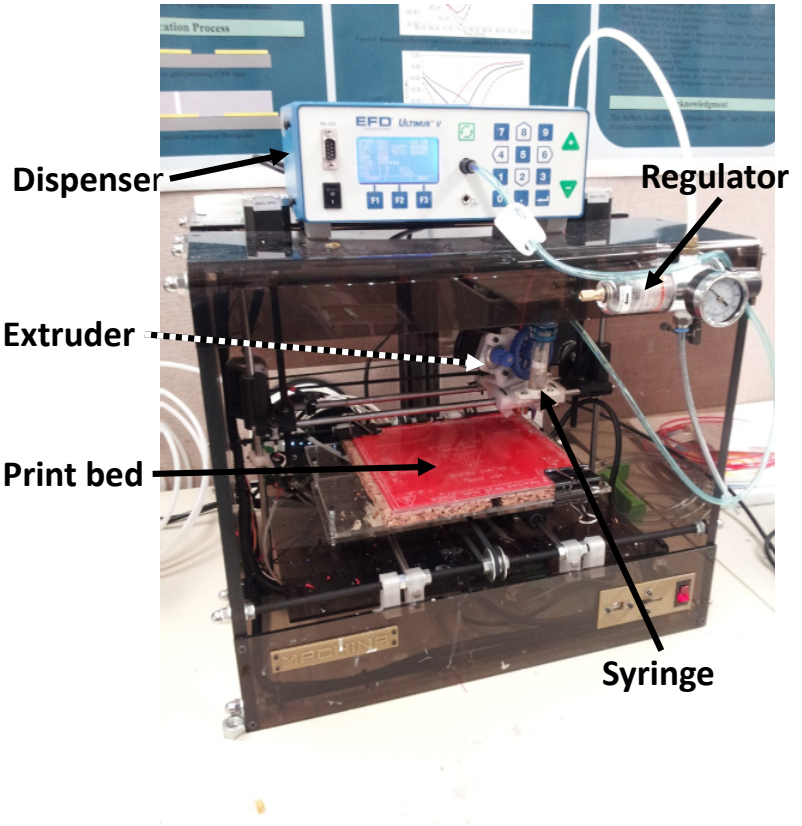
Dispenser
Regulator
Extruder
Print bed
Syringe

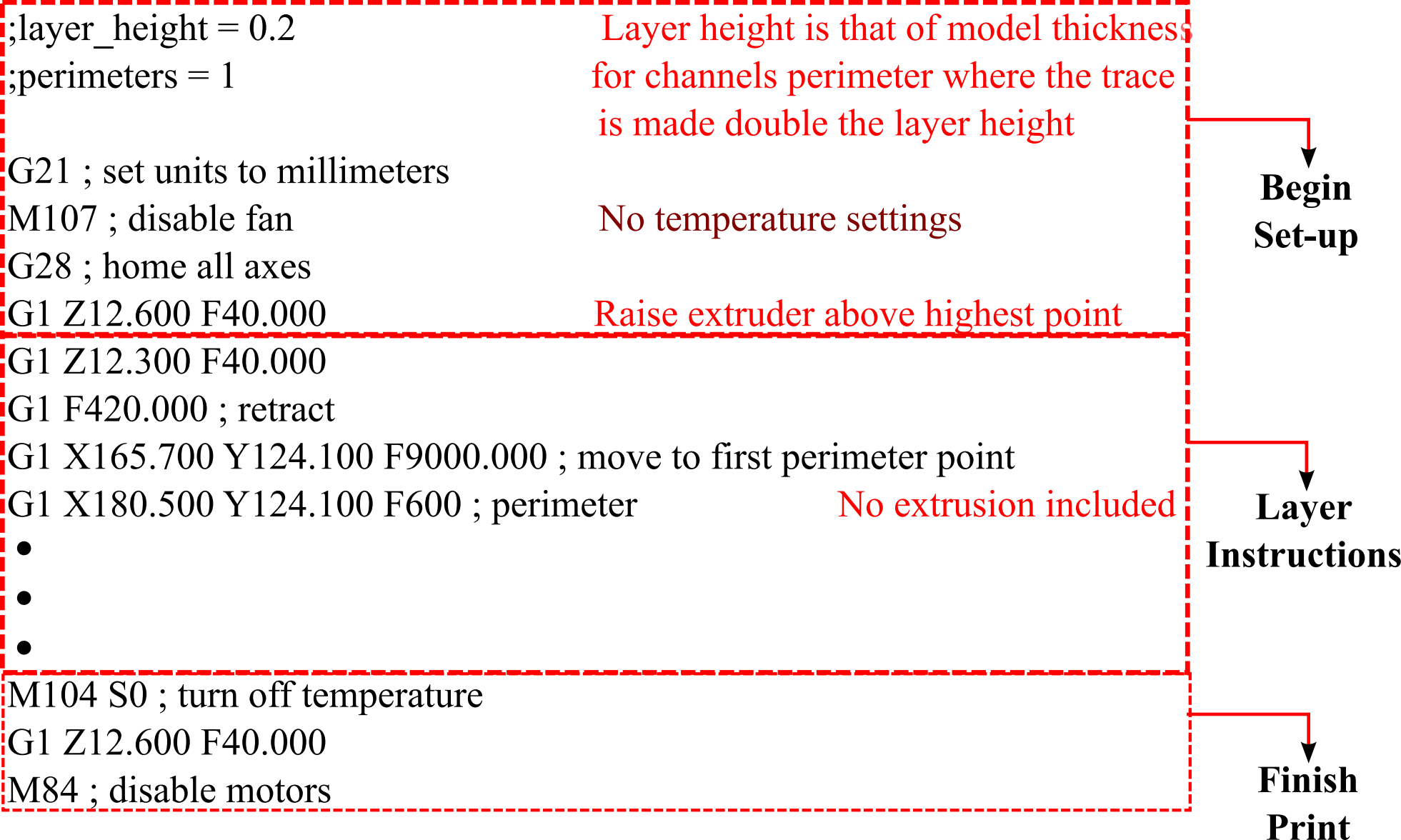
;layer_height = 0.2
;perimeters = 1
Layer height is that of model thickness for channels perimeter where the trace is made double the layer height
G21 ; set units to millimeters
M107 ; disable fan
No temperature settings
G28 ; home all axes
G1 Z12.600 F40.000
Raise extruder above highest point
Begin Set-up
G1 Z12.300 F40.000
G1 F420.000 ; retract
G1 X165.700 Y124.100 F9000.000 ; move to first perimeter point
G1 X180.500 Y124.100 F600 ; perimeter
No extrusion included
Layer Instructions
M104 S0 ; turn off temperature
G1 Z12.600 F40.000
M84 ; disable motors
Finish Print

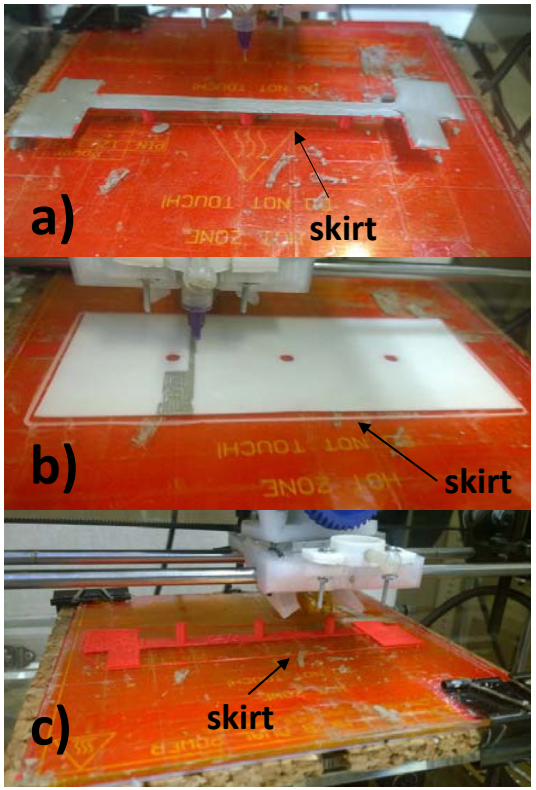
a)
skirt
b)
skirt
c)
skirt

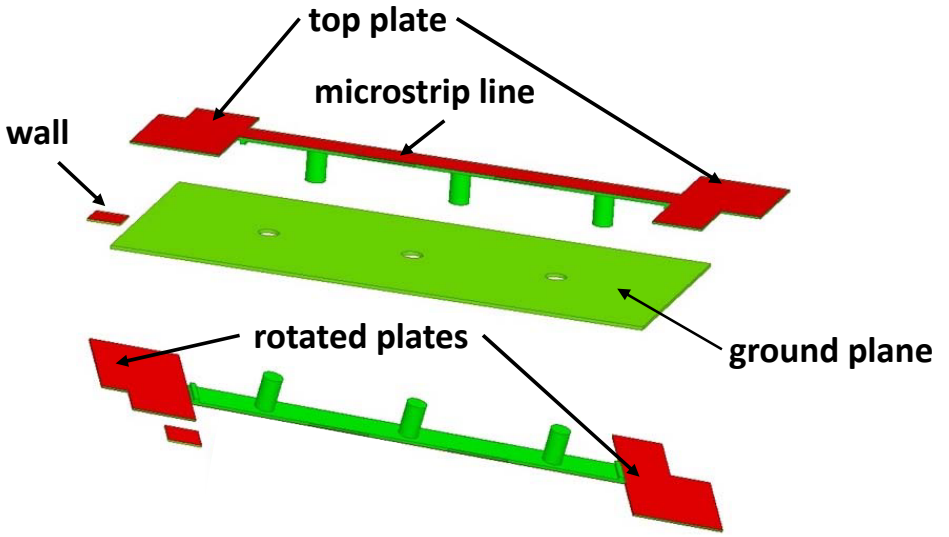
top plate
microstrip line
wall
rotated plates
ground plane

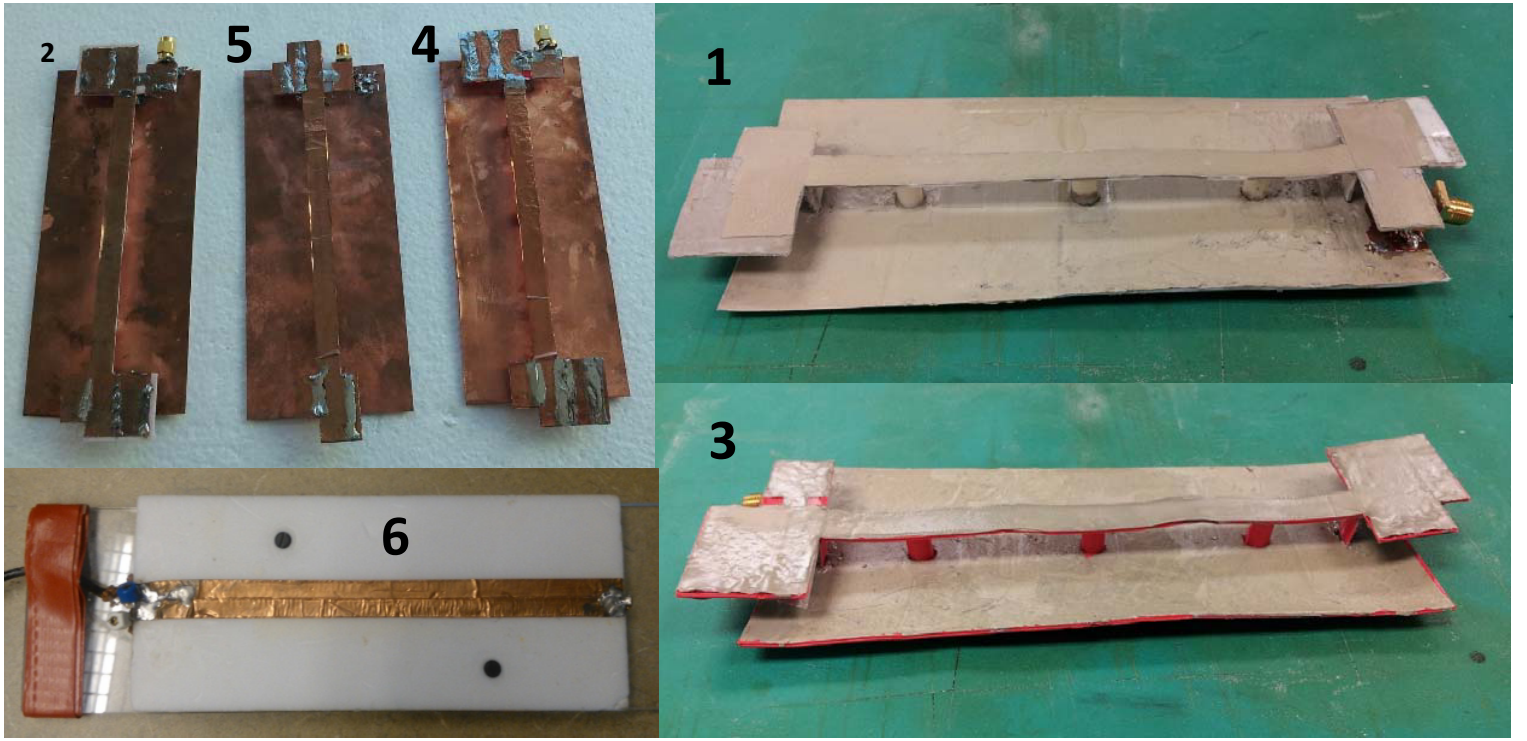
2
5
4
1
6
3

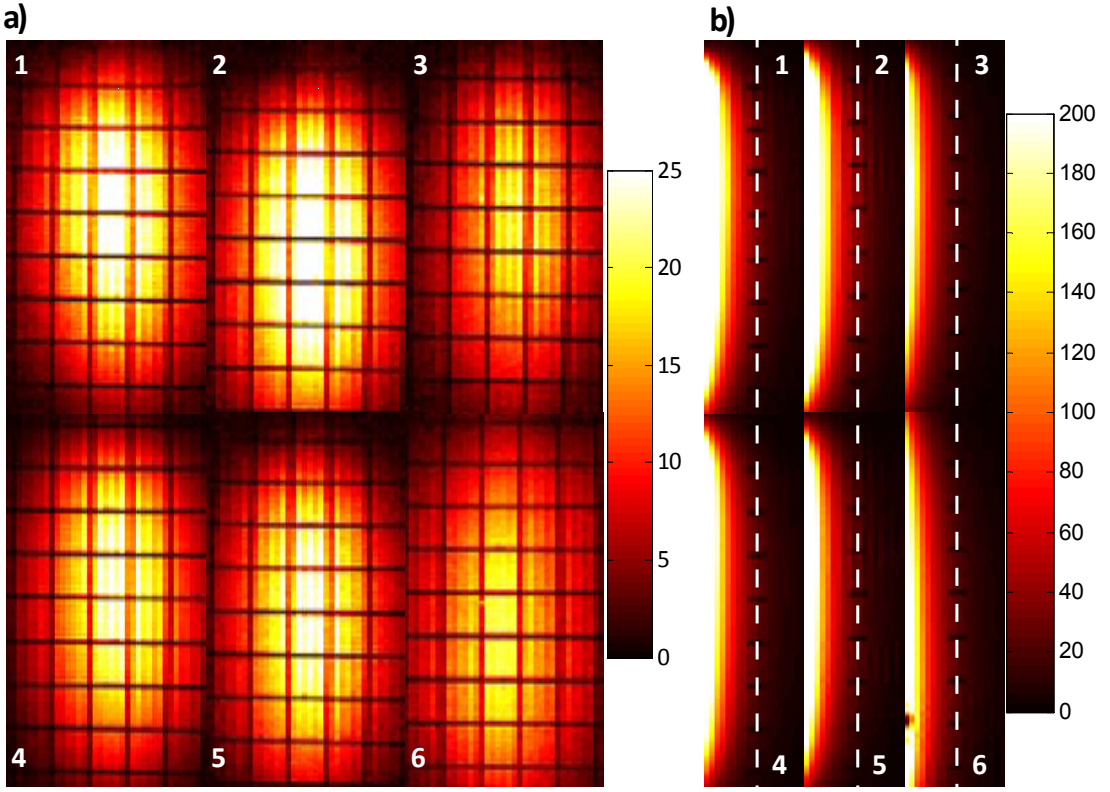
a)
1
2
3
4
5
6
25
20
15
10
5
0
b)
1
2
3
4
5
6
200
180
160
140
120
100
80
60
40
20
0